2020 International Symposium on Medical Robotics (ISMR)
Atlanta, GA, USA, November 18-20, 2020

A Wearable Anthropomorphically-Driven Prosthesis with a Built-In Haptic Feedback System

Ethan Miller[1], Ihemriorochi Amanze[2], and Jeremy Brown[3]

2020 International Symposium on Medical Robotics (ISMR) 978-1-7281-5488-6/20/$31.00 ©2020 IEEE DOI: 10.1109/ISMR48331.2020.9312933

***Abstract*— Recent developments in experimental anthropomorphically-driven prostheses have shown their potential as highly dexterous prosthetic devices. However, these prostheses are both unwearable and lack haptic feedback regarding antagonistic tensions. Here, we present a wearable, anthropomorphically-driven prosthesis with a built-in haptic feedback system. Two distinct control schemes were proposed and compared in a user study with N=6 able-bodied participants performing the Box and Blocks test.The first control scheme was designed to provide a more intuitive, human like actuation and relaxation of the hand, while the simpler controller was designed to reduce fatigue from sustaining EMG signals. Participants performed significantly better with lower fatigue levels while using the controller designed to be intuitive as opposed to the simpler controller. In addition, task performance with both controllers was better than reported performance with standard myoelectric prostheses. These findings suggest that there is potential utility in wearable anthropomorphically-driven prostheses, and provide support for future studies aimed at exploring the utility of haptic feedback in anthropomorphically-driven prostheses.**

Upper-limb prosthetics, Myoelectric prosthesis, Anthropomorphically-driven prosthesis, Prosthesis control scheme, Haptic feedback

I. Introduction

There are nearly 2 million people in the United States living with an amputation. Of these, 30% involve amputation of the upper extremity [1], [2]. Currently the standard of care is to fit these amputee with a prosthesis that utilizes body-power or electromyography to control flexion and extension of the prosthetic terminal device (hand). While body-powered terminal devices are typically limited to single-DoF actuation of two digits, advanced myoelectric terminal devices, such as the I-limb ultra revolution or the Michelangelo Hand, allow for multiple grip paradigms involving all five digits in a manner that mimics the natural hand [1].

Although these commercially available myoelectric terminal devices are designed to provide amputees with prostheses that emulate the form, function, and dexterity of an intact human hand [3], they often feature actuation schemes with high gear-ratios that limit an amputee's ability to modulate the hand's impedance. Yet, it is widely accepted that humans modulate the impedance of their limbs for various tasks [4]. There is even evidence to suggest that prosthesis users would modulate their device impedance for different tasks if allowed [5]. As a preliminary example, Brown *et al*. found that low-impedance prosthetic terminal devices allow grip/load force coordination in a manner consonant with the natural hand [6].

In an effort to allow control over the terminal device's impedance and to support more dexterous grasping movements, some experimental upper-limb prostheses use anthropomorphic actuation schemes [7]–[9].Note that anthropomorphically-driven prosthesis differ from other tendon driven prosthesis such as that used by Battaglia *et al*. [10] by allowing independent control over antagonistic tendons. Modeled after grasping functions of the human hand [8], these anthropomorphically-driven hands utilize complex structures and many individualized actuators to flex and extend the hand. Typically in these devices, each finger has artificial ligaments and tendons that mimic the anterior and posterior structure of the human hand. Xu *et al.* , for example, demonstrated that their biomimetic anthropomorphically-driven robotic hand was capable of reliable, human like, finger movements that endowed their hand with the ability to grasp a variety of objects [9]. Unfortunately, in order to achieve higher dexterity than commercially available prostheses, many of these anthropomorphically-driven hands use large and bulky actuation systems, making them unwearable [11]. This limits the range of tasks with which these devices can be tested.

Despite their novel control schemes, these anthropomorphic devices are no different than commercial prostheses in terms of haptic sensory feedback. In the natural hand, haptic feedback is necessary for fine dexterous control [12]. When antagonist muscles are actuated, the information about tension can be used to interpret the state of the hand [13]. The need for haptic information about antagonistic tensions is therefore unique to anthropomorphically-driven hands [12]. While there is evidence to suggest this information could provide utility in prosthesis control [12], there is a lack of research assessing the performance effects of feedback about tension in the control of anthropomorphically-driven prostheses.

In this manuscript, we present a wearable anthropomorphically-driven prosthesis capable of providing haptic-based tension feedback. We begin with a discussion of the design and functional operation of the prosthesis, including the haptic feedback system. We then describe two

*This work was not supported by any organization

[1]Ethan Miller is a Graduate Researcher in the Department of Biomedical Engineering at Johns Hopkins University, Baltimore, MD 21218, USA EthanDMiller06@gmail.com

[2]Ihemriorochi Amanze is a Junior High school student with the Ingenuity Project at Baltimore Polytechnic Institute, Baltimore, MD 21218, USA ihemamanze@gmail.com

[3]Jeremy Brown is with the Faculty of Mechanical Engineering at Johns Hopkins University, Baltimore, MD 21218, USA jdelainebrown@jhu.edu

unique control paradigms created for the prosthesis and the details of a small able-bodied user study designed to assess each controller's utility. We end with a discussion of the experimental findings from the user study in the broader context of prosthetic function.

II. Methods

Our experimental device, an anthropomorphically-driven prosthesis, was designed to incorporate two key features aimed at improving overall prosthesis functionality. First, the prosthesis features an anthropomorphic actuation paradigm that utilizes antagonistic tendons to separately control terminal device flexion and extension. Second, the prosthesis incorporates a unique haptic feedback system that utilizes skin-stretch to provide intuitive feedback regarding the amount of tension in either tendon. The device weighs 1.75Kg in total.

A. Device Design

This anthropomorphically-driven prosthesis (see Fig. 1) is comprised of a custom co-polymer prosthesis socket mated to an anthropomorphic terminal device via a Hosmer Quick Disconnect Wrist (USMC model). The custom socket is designed to be worn by able-bodied individuals on their right arm. The anthropomorphic terminal device is based on the open source bionic hand originally designed by Hendo [15]. Modifications have been made to improve cable routing through the fingers. Additional modifications allow compatibility with the Hosmer Quick Disconnect Wrist. The rubber bands on the anterior side of the original design were replaced with more tendon cabling to allow control over both flexion and extension. Each tendon cable originates at the finger tip, runs through the cable guides along the anterior and posterior sides of each finger, passes through the wrist cable guide, and terminates at a compression spring, which help return tendon cables to their resting position. Silicon (Dragon Skin 20) fingertips were designed for each finger to approximate the size of a human finger. All tendon cables connect to the far end of either the anterior or posterior compression spring, simplifying the actuation of the device to flexion and/or extension of all fingers simultaneously. In addition, actuation of both anterior and posterior tendons creates a bidirectional impedance of variable magnitude. An actuator tendon cable connects a compression spring to a rotary DC motor (Maxon RE30). The motors are mounted on the proximal end of the socket through two custom 3D printed motor mounts. Each motor features a rotary optical encoder (US Digital, 5000 CPR) to measure motor rotation.

Likewise, the haptic feedback system is based on the design originally proposed by Kayhan *et al*. [16] and has been integrated into the co-polymer socket. The haptic feedback system uses two servo motors (Tower Pro Micro servos MG90S) to create a pulling actuation on a proximal and distal band worn around the user's forearm as shown in Fig. 1. One servo motor is mounted onto the anterior side of the socket and is connected through cables to the anterior side of the bands. The other servo motor is mounted on the posterior side of the socket and is connected through cables

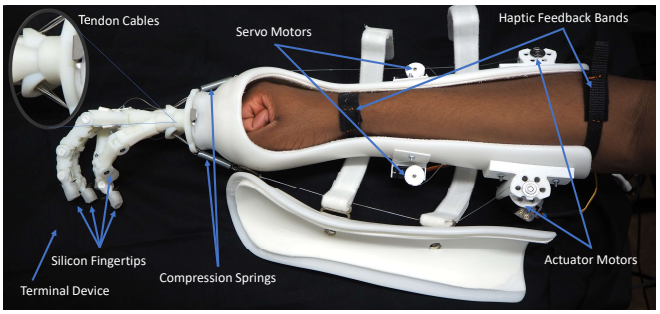

Fig. 1. The anthropomorphically-driven prosthesis with cover removed to show the haptic feedback bands around the user's forearm.

to the posterior side of the bands. Feedback is generated by activating the motors to pull on the anterior or posterior sides of the proximal and distal bands in proportion to the command signal sent to the DC motors controlling the anterior and posterior tendon cables. In this way, the user is provided haptic information regarding the amount of tension in the respective actuator tendon cables.

EMG signals were recorded from the wrist flexor and extensor muscle groups of the right forearm using a Delsys Bagnoli 16-channel EMG system with two surface electrodes and a ground electrode on the elbow. EMG calibration, normalization, and offset methods are consistent with those in [17] and are briefly described in Section II-C.1 below.

The two DC actuator motors were driven by a 3.5A linear current amplifier (Quanser AMPAQ-L4) with an amplification of 1V/A. Data acquisition and control were implemented through a Quanser Q8-USB data acquisition board(DAQ) operating at a 1 kHz sample rate. The whole system is controlled by a Dell Precision T5810 desktop running MATLAB R2017a. The Simulink Desktop Realtime Environment works in conjunction with Quanser's QUARC realtime block set.

B. Control Strategies

Terminal device flexion and extension were controlled by flexion and extension EMG signals under one of two control strategies, ALPHA or BETA. For both control strategies, EMG signals from the flexor muscles control activation of the actuator motor on the anterior sides of the prosthetic socket. Similarly, EMG signals from the extensor muscles control activation of the actuator motor on the posterior side of the prosthetic socket.

Controller ALPHA was designed to lower the effort of sustaining EMG signals while manipulating objects. In this trigger-based scheme, only a quick EMG spike of the desired magnitude is needed to proportionally activate the actuator motor. Likewise, a second EMG spike from the same muscle deactivates the actuator motor. Thus, the user can easily control flexion and extension separately while also maintaining the ability to activate both actuators and modulate the terminal device's impedance. The control law governing flexion and extension in the ALPHA control scheme is:

$$M_{flex} = \begin{cases} max(S_{flex\,off} \cdot K_{flex\,A}),\ \gamma_{flex} = 1 \\ 0,\ \gamma_{flex} = 0 \end{cases} \quad (1)$$

$$M_{ext} = \begin{cases} max(S_{ext\,off} \cdot K_{ext\,A}), \ \gamma_{ext} = 1 \\ 0, \ \gamma_{ext} = 0 \end{cases} \quad (2)$$

Where $S_{flex\,off}$ and $S_{ext\,off}$ are the normalized offset EMG signals, $K_{ext\,A}$ and $K_{flex\,A}$ are the proportional gains of the controller, and γ_{ext} and γ_{flex} are a binary variables whose value changes only if $S_{ext\,off}$ or $S_{flex\,off}$ respectfully go from a negative to positive value.

Fig. 4a shows a signal flow diagram describing the behavior of controller ALPHA. Here, U_p and U_p^2 describe the max function in (1) and (2) and γ is depicted as a switch. In addition, the motor command signals are saturated to control the minimum and maximum current sent to the motors, ensuring the device won't draw too much current from the amplifier. Fig. 2 provides an illustration of the controller behavior.

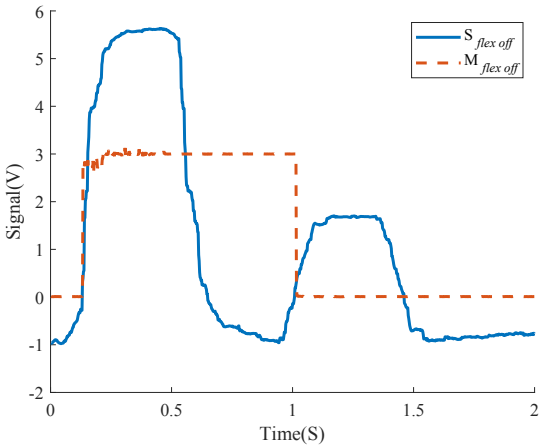

Fig. 2. An example plot of the flexor EMG signal $S_{flex\,off}$ and the corresponding motor command signal M_{flex} for controller ALPHA.

Controller BETA was designed to provide more intuitive control of the prosthesis. In this scheme, each motor output is proportional to the maximum respective EMG signal recorded while that EMG signal is above zero. When both EMG signals drop below their respective relaxation thresholds both motors relax. Thus, the user can antagonistically activate both actuators by simultaneously flexing, extending, and maintaining at least one EMG signal above the relaxation threshold. The control law governing flexion and extension in the BETA control scheme is

$$M_{flex} = \begin{cases} max(S_{flex\,off} \cdot K_{flex\,B}), \ \mathrm{S}_{flex\,off} > 0 \\ 0, \ S_{ext\,off} < T_{ext} \,\&\, S_{flex\,off} < T_{flex} \\ M_{flex,prev}, \ otherwise \end{cases} \quad (3)$$

$$M_{ext} = \begin{cases} max(S_{ext\,off} \cdot K_{ext\,B}), \ \mathrm{S}_{ext\,off} > 0 \\ 0, \ S_{ext\,off} < T_{ext} \,\&\, S_{flex\,off} < T_{flex} \\ M_{ext,prev}, \ otherwise \end{cases} \quad (4)$$

where $S_{flex\,off}$ and $S_{ext\,off}$ are the normalized offset EMG signals, $K_{flex\,B}$ and $K_{ext\,B}$ are the proportional gains of the controller, and T_{flex} and T_{ext} are the relaxation thresholds.

Fig. 4b shows the signal flow diagram describing the behavior of controller BETA. Here U_p and U_p^2 describe the max function in (3) and (4). In addition, the motor command signals are saturated as with controller ALPHA. Fig. 3 provides an illustration of the controller behavior.

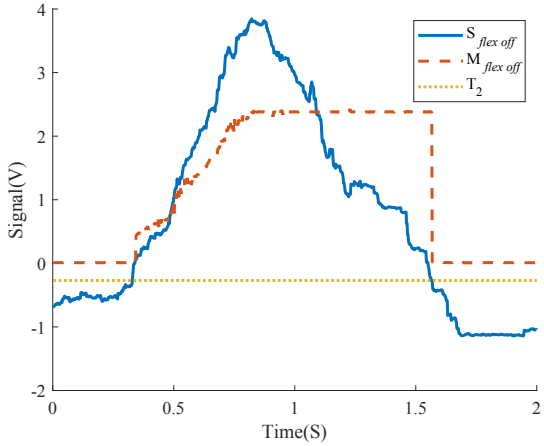

Fig. 3. An example plot of the flexor EMG signal $S_{flex\,off}$ and the motor command signal M_{flex} for controller BETA. Note, the extensor EMG signal $S_{ext\,off} < T_{ext}$.

C. Experimental Procedure

To evaluate the utility of each control strategy, we investigated the ability of N=6 able-bodied participants (five male, one female) ages 27.5 ± 11 (all participants above 18) to perform the Box and Blocks test [14]. This test is often used to assess manual dexterity in individuals with neurological disorders [14], and has been used to assess prosthesis function as well [18]–[21]. The duration of the experiment was approximately 60 minutes and participants were compensated at a rate of $10 per hour. All participants were consented according to a protocol approved by the Johns Hopkins School of Medicine Institutional Review Board (Study# IRB00147458). Participants were randomized into two groups (A and B). Participants in group A performed the task with controller ALPHA followed by controller BETA. Participants in group B performed the task with controller BETA followed by controller ALPHA. For this experiment, no haptic feedback was provided.

1) Setup and Training: After providing informed consent, participants sat on a stool facing a table where the experiment would take place. One electrode was placed over the participant's right wrist flexor muscle group and another electrode was placed over the right wrist extensor muscle group. The optimal location in these muscle groups was located by palpating the participant's forearm while they flexed and extended their wrist. A ground electrode was then placed over the participant's right elbow. A compression sleeve covered the participant's right arm to keep the the electrodes from shifting. Medical tape was gently wrapped around participant's bicep and the wires to prevent tugging.

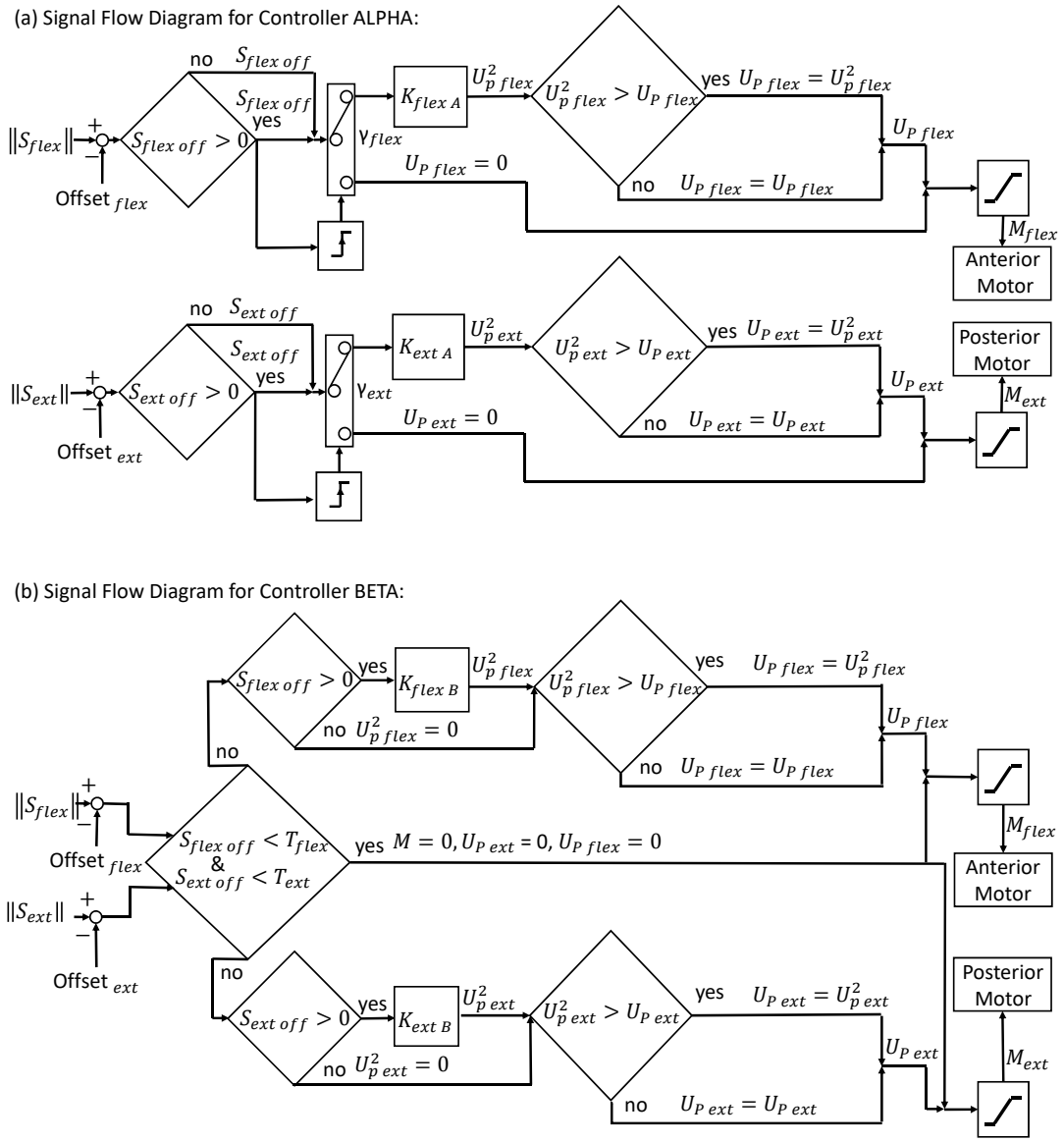

Fig. 4. The signal flow diagrams for the two control strategies, ALPHA (a) and BETA (b).

Participants were then asked to hold their arm in the air for calibration. After a two second baseline reading, participants were asked to flex and relax their wrist in one second intervals for eight seconds while the system calibrated the minimum, maximum, and offset values for the flexor EMG signal $S_{flex\,off}$. This was then repeated for wrist extension to calibrate the extensor EMG signal $S_{ext\,off}$. Participants were instructed on the best practices for producing clear EMG signals. When controlling the prosthesis, the raw EMG signals were rectified and smoothed by taking the RMS over a 200 ms window. Additionally, the signals were normalized and offset to provide the desired input to the controller.

After calibration, participants were then informed of the control method they would be using first (based on group randomization). Participants were then instructed to place their right arm in the prosthetic socket. Additional manual adjustment was used to fine tune parameters until participants were able to repeatedly flex and extend the prosthesis with low, medium, and high tension and participants felt comfortable with the device's response to their EMG commands. Once appropriate control was achieved, participants were provided instructions on performance of the Box and Blocks test. Then, as practice, participants were instructed, without time constraint, to move five blocks over the barrier and release them into the second compartment. If needed, further adjustment of parameters was performed.

2) Protocol: Following setup and training, participants performed eight trials of Box and Blocks test using their designated controller. In each trial, participants were given 60 seconds to move as many blocks as possible from the right compartment of the task to the left. Participants were given a 45 second rest between each trial and were allowed more

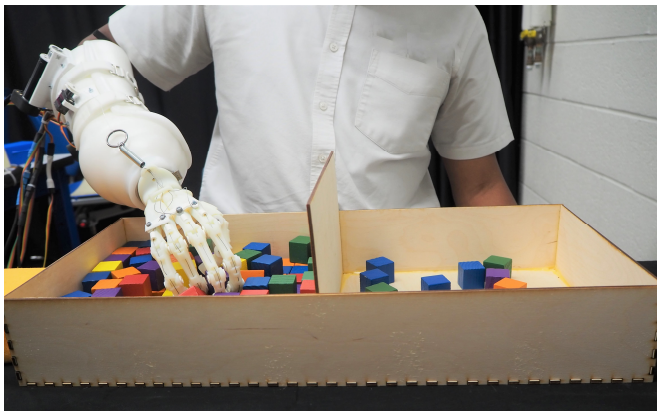

Fig. 5. Experimental setup of Box and Blocks test.

rest time upon request. Before the first trial and after each consecutive trial, participants were asked to rank their arm fatigue on a scale from one to ten, with ten corresponding to the inability to move their arm. After completing eight trials with the first controller, participants were given time to rest while they completed a short survey regarding their perception of the controller and their ability to move blocks. Then the control method was switched to the opposite controller. Some additional manual adjustment of parameters was performed to ensure adequate control. Participants then practiced once again by moving 5 blocks over the barrier. After practice, participants were asked to rank their fatigue and allowed to rest until it returned to within one point of their previous baseline from the first controller. Participants performed eight trials of the task with the new controller using the same rest intervals. Fatigue scores were recorded after each trial. After completing the second set, participants were asked to fill out the remainder of the survey regarding their perception the second controller, their ability to move blocks with the controller, a demographic survey, and a final survey asking them to compare how intuitive the two controllers were. Finally, participants were given time to add any additional comments about their experience.

D. Metrics and Statistical analysis

The two quantitative metrics used in this study to evaluate the two controllers include the block transfer rate and the block transfer efficiency. The block transfer rate is calculated as the number of blocks moved in the 60-second trial. The block transfer efficiency is calculated as the number of blocks moved per total sum of terminal device flexions and extensions in the 60-second trial. In addition, survey responses for fatigue and participant's controller preference were used for qualitative assessment.

Statistical analysis was carried out in MATLAB 20184a. First, data sets were tested for normality, homogeneity of variance, and sphericity using the Lilliefors test, the Bartlett test, and the Mauchly's test, respectively. A Wilcoxon Signed-Rank test was used on the block transfer efficiency, the block transfer Rate, and the survey data along with fatigue scores to determine the differences between ALPHA and BETA. Both p values and effect sizes (r) are reported when possible.

III. Results

All data was analyzed using non-parametric statistical analysis after failing to pass the normality test. During experimentation, the experimental apparatus malfunctioned on four trials. When this occurred, the device and task were reset and the trial was rerun. These malfunctions only affected participants two and three. In addition, participant five noted in their survey that they significantly changed their block grasping and moving strategy to improve performance in the last trial while using controller ALPHA which significantly increased their performance compared to prior trials.

A. Block Transfer Rate

Overall, the Wilcoxon Signed-Rank test showed participants moved significantly more blocks per minute with controller BETA than with controller ALPHA (p = 3.20e-08, r = -0.80) (see Fig. 6). Participants moved an average of 6 $\pm$3.49 blocks per minute when using controller ALPHA and an average of 11$\pm$2.37 per minute with controller BETA.

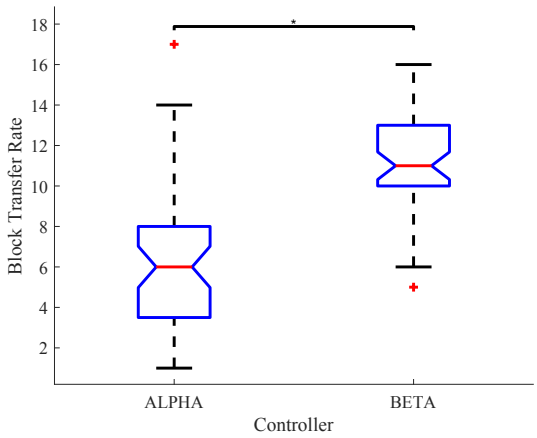

Fig. 6. Box plot of Box and Blocks test results for controllers ALPHA and BETA.* indicates p $<$ 0.05.

B. Block Transfer Efficiency

Overall, the Wilcoxon Signed-Rank test showed participants were significantly more efficient with controller BETA than with controller ALPHA (p = 2.27e-08, r = -0.81) as seen in Fig. 7. The average block transfer efficiency for controller ALPHA was 0.22$\pm$0.15, and the average block transfer efficiency for controller BETA was 0.41 $\pm$0.13.

C. Survey

The Wilcoxon Signed-Rank test showed participants expressed significantly lower fatigue levels while using controller BETA than they did with controller ALPHA (p value = 0.022, r = 0.33). Additionally,the Wilcoxon Signed-Rank test showed participants overall preferred controller BETA and felt more confident in their ability to move blocks when using controller BETA (p= 0.0015). All participants but one found controller BETA to be more intuitive.

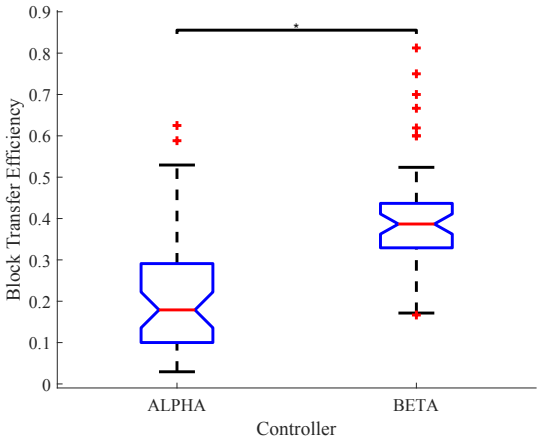

Fig. 7. Box plot of efficiency results for controllers ALPHA and BETA.* indicates $p < 0.05$.

IV. Discussion

In this study, we presented an anthropomorphically-driven prosthesis that features a tension-based haptic feedback system and the results of a small user study designed to evaluate and compare two competing control strategies. This prosthesis was designed to allow independent control over extension and flexion of the terminal device. Controller ALPHA was designed to minimize the user's EMG activations and therefore fatigue. Alternatively, controller BETA was designed as a more intuitive approach. Overall, controller BETA allowed for better task performance both in terms of the block transfer rate and the block transfer efficiency, and was participants' preferred control strategy.

The superiority of controller BETA is likely due to its intuitive nature, where muscle signals correspond more directly with motor control. Alternatively, controller ALPHA sustained device actuation, which allowed participants to relax EMG signals, but participants reported less fatigue with controller BETA than with controller ALPHA. Thus, controller BETA seems to stand out as a more effective way to control this device.

It is also worth considering how task performance with this prosthesis compares to task performance with other prostheses and prosthesis control schemes. Table I highlights the average Box and Blocks test scores from participants using their dominant right hand as well as various prostheses. The table also includes data from some able bodied subjects as well as some amputees. Note, some scores have been adjusted to reflect the 1 minute trials used in this study.

While the training periods and number of trials vary for the Box and Blocks test scores reported in Table I, these scores provide insight into the current level of manual dexterity in prostheses. Our anthropomorphically-driven prosthesis resulted in higher mean scores than some records for standard myoelectric prostheses with both controllers (ALPHA and BETA). Additionally, under controller BETA, participants with this anthropomorphically-driven prosthesis also scored higher on average than some targeted muscle reinnervation prosthesis users. At the same time, the Michelangelo prosthesis seems to greatly outperform any other prosthesis, likely due to the six months of training provided. Body-powered prostheses also tend to outperform myoelectric prostheses. It's possible that the scores for our anthropomorphic prosthesis might improve when the haptic feedback system is engaged.

TABLE I

Reported Box and Blocks scores for various types of prostheses.

Conditions	Blocks per Minute	Source
Female dominant right hand	86 ± 7.4	[14]
Custom body-powered prosthesis	$15 - 20$	[18]
Standard myoelectric prosthesis	$\approx 3 \pm 2.5^{**}$	[19]
TMR* prosthesis	$\approx 8 \pm 4.5^{**}$	[19]
Hosmer hook prosthesis	22.7	[20]
Michelangelo prosthesis	29.3 ± 3.20	[21]
ALPHA (this manuscript)	6 ± 3.49	N/A
BETA (this manuscript)	11 ± 2.37	N/A

*Targeted muscle reinnervation ** Approximated from graphic

While these results show promise for anthropomorphically-driven prosthesis, the current device has limitations that should be addressed going forward. First, despite its wearability, the device is highly cumbersome. The weight of the motors and the need for precise EMG signals can be mentally and physically exhausting. Participants reported high fatigue scores very early in the experiment and this likely affected their performance throughout the trials. Second, the short practice period for each controller may have resulted in unbalanced learning. While some participants may have learned quickly, others were learning throughout the experiment. Third, participants had different arm sizes and the custom socket did not fit all participants snugly, even with the compression sleeve. This caused the device to slightly shift on their arms as they performed the task. Fourth, the built-in haptic feedback system was not used in this experiment and thus comparison of the effect haptic feedback has on each control method was not explored. Finally, only able-bodied participants were tested in this experiment. Despite these limitations, however, we feel that the work presented here provides a foundation for future studies focused on investigating wearable anthropomorphically-driven prostheses.

Acknowledgment

Our team would like to thank Dankmeyer, Inc. for casting the custom socket and providing the Hosmer Quick Disconnect. We would also like to thank Maya Sitaram, Mohit Singhala, and Garret Ung for their support and help throughout the project.

References

[1] A. Sabzi Sarvestani and A. Taheri Azam, "Amputation: A Ten-Year Survey," Trauma Mon, vol. 18, no. 3, pp. 126–129, Dec. 2013.

[2] C. Toledo, L. Leija, R. Munoz, A. Vera, and A. Ramirez, "Upper limb prostheses for amputations above elbow: A review," in 2009 Pan American Health Care Exchanges, 2009, pp. 104–108.

[3] F. Cordella et al., "Literature Review on Needs of Upper Limb Prosthesis Users," Front Neurosci, vol. 10, May 2016.

[4] N. Hogan, "Adaptive control of mechanical impedance by coactivation of antagonist muscles," IEEE Transactions on Automatic Control, vol. 29, no. 8, pp. 681–690, Aug. 1984.
[5] A. A. Blank, A. M. Okamura, and L. L. Whitcomb, "Task-dependent impedance and implications for upper-limb prosthesis control," The International Journal of Robotics Research, vol. 33, no. 6, pp. 827–846, May 2014.
[6] J. D. Brown et al., "An exploration of grip force regulation with a low-impedance myoelectric prosthesis featuring referred haptic feedback," Journal of NeuroEngineering and Rehabilitation, vol. 12, no. 1, p. 104, Nov. 2015.
[7] C. Li, X. Gu, X. Xiao, G. Zhu, A. V. Prituja, and H. Ren, "Transcend Anthropomorphic Robotic Grasping With Modular Antagonistic Mechanisms and Adhesive Soft Modulations," IEEE Robotics and Automation Letters, vol. 4, no. 3, pp. 2463–2470, Jul. 2019.
[8] Z. Xu, Y. Matsuoka, and A. D. Deshpande, "Crocheted artificial tendons and ligaments for the anatomically correct testbed (ACT) hand," in 2015 IEEE International Conference on Robotics and Biomimetics (ROBIO), 2015, pp. 2449–2453.
[9] Z. Xu and E. Todorov, "Design of a highly biomimetic anthropomorphic robotic hand towards artificial limb regeneration," in 2016 IEEE International Conference on Robotics and Automation (ICRA), 2016, pp. 3485–3492.
[10] E. Battaglia, J. Clark, M. Bianchi, M. Catalano, A. Bicchi, and M. K. O'Malley, "Skin stretch haptic feedback to convey closure information in anthropomorphic, under-actuated upper limb soft prostheses," IEEE Transactions on Haptics, pp. 1–1, 2019.
[11] S. B. Godfrey, A. Altobelli, M. Rossi, and A. Bicchi, "Effect of homogenous object stiffness on tri-digit grasp properties," in 2015 37th Annual International Conference of the IEEE Engineering in Medicine and Biology Society (EMBC), 2015, pp. 6704–6707.
[12] I. Williams and T. G. Constandinou, "Modelling muscle spindle dynamics for a proprioceptive prosthesis," Conf Proc IEEE Eng Med Biol Soc, vol. 2013, pp. 1923–1926, 2013.
[13] C. Xiong, W. Chen, B. Sun, M. Liu, S. Yue, and W. Chen, "Design and Implementation of an Anthropomorphic Hand for Replicating Human Grasping Functions," IEEE Transactions on Robotics, vol. 32, no. 3, pp. 652–671, Jun. 2016.
[14] V. Mathiowetz, G. Volland, N. Kashman, and K. Weber, "Adult Norms for the Box and Block Test of Manual Dexterity," Am J Occup Ther, vol. 39, no. 6, pp. 386–391, Jun. 1985.
[15] J. Hendo, "3D Printed Bionic Hand Skeleton," Instructables. [Online]. Available: https://www.instructables.com/id/3D-Printed-Bionic-Hand-Skeleton/. [Accessed: 1-June-2019].
[16] O. Kayhan, A. K. Nennioglu, and E. Samur, "A skin stretch tactor for sensory substitution of wrist proprioception," in 2018 IEEE Haptics Symposium (HAPTICS), 2018, pp. 26–31.
[17] N. Thomas, G. Ung, C. McGarvey, and J. D. Brown, "Comparison of vibrotactile and joint-torque feedback in a myoelectric upper-limb prosthesis," J NeuroEngineering Rehabil, vol. 16, no. 1, p. 70, Jun. 2019.
[18] K. D. Gemmell, M. T. Leddy, J. T. Belter, and A. M. Dollar, "Investigation of a passive capstan based grasp enhancement feature in a voluntary-closing prosthetic terminal device," in 2016 38th Annual International Conference of the IEEE Engineering in Medicine and Biology Society (EMBC), 2016, pp. 5019–5025.
[19] L. A. Miller, K. A. Stubblefield, R. D. Lipschutz, B. A. Lock, and T. A. Kuiken, "Improved Myoelectric Prosthesis Control Using Targeted Reinnervation Surgery: A Case Series," IEEE Transactions on Neural Systems and Rehabilitation Engineering, vol. 16, no. 1, pp. 46–50, Feb. 2008.
[20] J. T. Belter, M. T. Leddy, K. D. Gemmell, and A. M. Dollar, "Comparative clinical evaluation of the Yale Multigrasp Hand," in 2016 6th IEEE International Conference on Biomedical Robotics and Biomechatronics (BioRob), 2016, pp. 528–535.
[21] M. Luchetti, A. G. Cutti, G. Verni, R. Sacchetti, and N. Rossi, "Impact of Michelangelo prosthetic hand: Findings from a crossover longitudinal study," J Rehabil Res Dev, vol. 52, no. 5, pp. 605–618, 2015.